Study of Enzymatic G6P Synthesis Using Polymer-Bound ATP in Membrane Reactors

Wael Abdelmoez, Kosaku Ishimi, and Haruo Ishikawa
Dept. of Chemical Engineering, Osaka Prefecture University 1-1 Gakuen-cho, Sakai, Osaka 599-8531, Japan

DOI 10.1002/aic.10649
Published online September 15, 2005 in Wiley InterScience (www.interscience.wiley.com).

The performance of membrane reactors, in which the enzymatic synthesis of glucose 6-phosphate from glucose and polymer-bound cofactor ATP with simultaneous regeneration of polymer-bound ATP from polymer-bound ADP and acetyl phosphate are performed, was analyzed theoretically. Simplified and realistic models for two different membrane reactors, a plug-flow–type membrane reactor (PFMR) in a diffusion mode and a continuous stirred tank reactor–type membrane reactor (CSTMR) in a filtration mode, were presented and compared theoretically. The results showed that the reactor performance mainly depends on the operating conditions and that, in most cases, the PFMR in a diffusion mode was found to be superior to the CSTR in a filtration mode. This study provides useful information for selecting and optimizing of the reactor for enzymatic reactions requiring cofactors. © 2005 American Institute of Chemical Engineers *AIChE J,* 52: 683–691, 2006

Keywords: membrane reactor performance, glucose 6-phosphate synthesis, polymer-bound ATP, ATP regeneration

Introduction

Enzymatic syntheses often need not only enzymes as a catalyst but also a stoichiometrically equivalent amount of low molecular mass cofactors, which are quite expensive. The biosyntheses that require adenosine triphosphate (ATP) represent an example of cofactor-dependent systems and need a continuous regeneration of ATP to be industrially feasible. Of the methods available for the regeneration of ATP, the enzymatic method has been chosen to be the most suitable route for industrial applications.[1,2]

Membrane reactors are believed to constitute the best reactor system for carrying out enzymatic reactions requiring cofactor. The potential applications of such reactors have been reviewed and reported by Belfort[3] and Prazeres and Cabral.[4]

Two types of membrane reactor with different operation mode have been used. The first one is a plug-flow–type membrane reactor (PFMR)[5-12] and the other, a continuous stirred tank–type membrane reactor (CSTMR).[13,14] The PFMR is further subclassified in accordance with its operation mode: diffusion and filtration modes. Reactor performances of these operation modes were compared and their advantages and limitations were reported in the case of a single enzymatic reaction with one substrate, lactose hydrolysis by β-galactosidase.[15] It was reported that the performance of the PFMR in a diffusion mode was the same as that of a typical plug-flow reactor. However, the performance of the PFMR in a filtration mode was identical to that of the CSTMR.[7,8,16] Furthermore, the performance of the CSTMR was found to deteriorate rapidly as a result of inactivation of enzymes by the shear stress or sedimentation on the membrane.[14,15]

The bottleneck for the economical application of the abovementioned membrane systems lies in the specific retention of the enzymes and cofactor within continuous reactor systems as well as the operation modes of such reactors. Both native and polymer-bound cofactors were regenerated in membrane reactors with different configurations and characteristics. An ultrafiltration membrane, with a low molecular mass cutoff of 0.5–0.7 kDa, was used to retain native cofactors.[5,6] However, this type of membrane offers poor performance characteristics

Correspondence concerning this article should be addressed to W. Abdelmoez at drengwael2003@yahoo.com.

and low permeability of substrate and/or product. Alternatively, a negatively charged ultrafiltration membrane with a molecular mass cutoff of 1 kDa was used[17-19] to improve the performance and prevent membrane fouling with negatively charged enzymes. However, the need to retain charged components limits their use. An ultrafiltration membrane with much higher molecular cutoff (10–13 kDa)[14] was used to enhance the reactor performance and to overcome the disadvantageous of using a membrane with very low molecular mass cutoff. In this case, the molecular mass of native cofactors has to be increased so that the ultrafiltration membrane can retain them.

Although numerous theoretical analyses of such reactors have been presented in the literature, in every case, the reaction has been limited to one substrate system. However, in the case of coupled reactions the situation is somewhat complicated and both the reactor size and distribution of the reaction products are affected by the type of reactor and the operation mode. In our laboratory, native ATP regeneration during glucose 6-phosphate (G6P) or fructose 1,6-diphosphate (FDP) production in the PFMR in a diffusion mode with continuous feeding of native ATP has been investigated both theoretically and experimentally in two independent studies.[9-12] The simulation results elucidated the effects of the reactor configurations and various operational conditions on the conversion of glucose, the ATP recycle number, and the space–time yield of the products. The experimental results were proved to be in good agreement with the theoretical predications.

From the investigations reviewed above, it became clear that intensive studies focusing on the performance of the reactors in the case of using polymer-bound cofactors should be carried out. Therefore, in this work a theoretical study was performed to develop an efficient membrane reactor system in which enzymatic G6P synthesis from glucose and polymer-bound ATP and enzymatic polymer-bound ATP regeneration reaction take place simultaneously.

Theory

Reaction system

Enzymatic synthesis of G6P catalyzed by *Bacillus stearothermophilus* glucokinase (GK) and enzymatic regeneration of the polymer-bound ATP catalyzed by *B. stearothermophilus* acetate kinase (AK) in membrane reactors were studied theoretically. The overall reaction of the enzymatic G6P synthesis is expressed by

$$\text{Polymer-bound ATP} + \text{Glucose} \xrightarrow{\text{GK}} \text{Polymer-bound ADP} + \text{G6P} \quad (1)$$

The polymer-bound adenosine diphosphate (ADP) produced in reaction 1 reacts with acetyl phosphate can be converted to the polymer-bound ATP by the following reaction:

$$\text{Polymer-bound ADP} + \text{AcP} \overset{\text{AK}}{\rightleftharpoons} \text{Polymer-bound ATP} + \text{Acetate} \quad (2)$$

When native ATP and ADP are used, the rate equation of the reaction catalyzed by GK was derived in one of our previous studies[20] as follows:

$$\frac{v_{GK}}{[\text{GK}]_0} = \frac{\lambda C_1 C_5}{1 + \omega_1 C_1 + \omega_2 C_5 + \omega_3 C_1 C_5 + \omega_4 C_6 + \omega_5 C_6 C_1 + \omega_6 C_6 C_1 C_5} \quad (3)$$

where v_{GK} is the reaction rate (M s^{-1}), $[GK]_0$ is the initial GK concentration (M), C_1 is the glucose concentration (M), C_5 is the ATP concentration (M), C_6 is the ADP concentration (M), and λ and ω_j (j = 1–6) are the kinetic parameters consisting of the rate constants. The values of these parameters when native ATP and ADP are used were obtained in our previous work[21] and used in this work in the simulation.

The rate equation of the reaction catalyzed by AK was derived in one of our previous studies[22] as follows:

$$\frac{v_{AK}}{[\text{AK}]_0} = \frac{\begin{array}{r}\alpha_1 C_6 C_5 + \alpha_2 C_6^2 C_5 + \alpha_3 C_6 C_3^2 + \alpha_4 C_6 C_3 C_5 \\ + \alpha_5 C_6 C_3 C_4 + \alpha_6 C_6^2 C_3^2 + \alpha_7 C_6 C_3 C_5 C_4 \\ - \alpha_8 C_5 C_4 - \alpha_9 C_6 C_5 C_4 - \alpha_{10} C_3 C_5 C_4 \\ - \alpha_{11} C_5^2 C_5 - \alpha_{12} C_5 C_4^2 - \alpha_{13} C_5^2 C_4^2\end{array}}{\begin{array}{l}1 + \beta_1 C_6 + \beta_2 C_3 + \beta_3 C_5 + \beta_4 C_4 + \beta_5 C_6^2 + \beta_6 C_6 C_3 \\ + \beta_7 C_6 C_5 + \beta_8 C_6 C_4 + \beta_9 C_3^2 + \beta_{10} C_3 C_5 \\ + \beta_{11} C_3 C_4 + \beta_{12} C_5^2 + \beta_{13} C_5 C_4 + \beta_{14} C_4^2 \\ + \beta_{15} C_6^2 C_3 + \beta_{16} C_6 C_3^2 + \beta_{17} C_6 C_3 C_5 \\ + \beta_{18} C_6 C_3 C_4 + \beta_{19} C_6 C_5 C_4 + \beta_{20} C_3 C_5 C_4 \\ + \beta_{21} C_5^2 C_4 + \beta_{22} C_5 C_4^2 + \beta_{23} C_6^2 C_3^2 \\ + \beta_{24} C_6 C_3 C_5 C_4 + \beta_{25} C_5^2 C_4^2\end{array}} \quad (4)$$

In Eq. 4, C_3 is the acetyl phosphate (AcP) concentration (M), C_4 is the acetate concentration (M), C_5 is the ATP concentration (M), and C_6 is the ADP concentration (M). α_j (j = 1–13) and β_j (j = 1–25) are the kinetic parameters consisting of the rate and equilibrium constants. The values of these parameters when native ATP and ADP are used were obtained in our previous work[21] and used in this work in the simulation.

Recently, we succeeded in synthesizing the polymer-bound ATP and ADP by binding native ATP and ADP to a carboxy-terminated polyamidoamine dendrimer.[23] When the polymer-bound ATP and ADP were used as cofactors, the rates of reactions catalyzed by *B. stearothermophilus* GK and AK were well correlated by the same rate equations as shown above (Eqs. 3 and 4), with kinetic parameters different from those obtained when native ATP and ADP are used.[24,25] In the literature, it was reported that many kinds of polymer-bound ATPs and ADPs have been synthesized with having different kinetic parameters.[26] Accordingly, even though the polymer-bound ATP and ADP were used as cofactors in the present simulation (the kinetic parameters of which we previously measured[24,25]), we decided to use the values of the kinetic parameters of the native ATP and ADP. The reason behind that is to cancel the effect of the difference in the kinetics properties between native and the polymer-bound ATP and ADP. In this way, the difference in simulation results between the systems that used native ATP or polymer-bound ATP is attributed to differences in the reactor performance in each case. Accord-

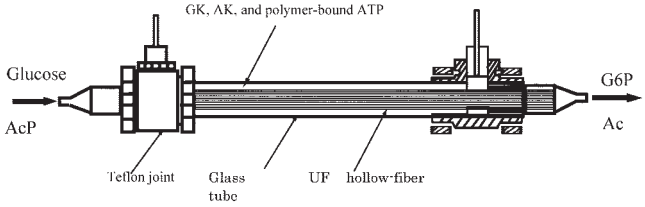

Figure 1. Illustration of the plug-flow–type hollow-fiber membrane reactor in a diffusion mode.

ingly, such treatment will lead to a general conclusion that could be applied to any enzymatic reaction systems requiring cofactors.

Reactor models

In this work, the performances of two different reactors were analyzed. The first one is the PFMR in a diffusion mode and the other, the CSTMR in a filtration mode. The results will be reported emphasizing the comparison between the performances of the two different reactors under the experimental or operating conditions where the best reactor performance can be expected.

Plug Flow-Type Membrane Reactor in a Diffusion Mode. The enzymatic G6P or FDP production and simultaneous regeneration of native ATP in the PFMR in a diffusion mode, which has almost the same structure as shown schematically in Figure 1, have been investigated both theoretically and experimentally in two independent studies.[9-12] The good agreement between the experimental results and the theoretical predictions in the cases of production of both G6P and FDP confirmed the validity of the models used. Therefore, in the present work we adopted a similar analytical model, which was modified for the predictions of the performance of the continuous enzymatic production of G6P using the polymer-bound ATP in the PFMR in a diffusion mode.

The PFMR in a diffusion mode used in this work consisted of a glass tube (ID 1.0 cm), in which seven asymmetric ultrafiltration hollow-fiber tubes (molecular mass cutoff of 13,000) were packed. Both ends of each fiber were connected to stainless steel pipes (OD 1.0 mm; length 5 cm), and these pipes were joined with epoxy resin into a bundle. The specifications of the reactor are given in Table 1.

A schematic illustration of the mass transfer of all the components involved in the reactions and the overall reactions is shown in Figure 2. The enzymes, GK and AK, and the polymer-bound ATP (and ADP) are confined in the shell-side space, and a buffer solution containing substrate glucose and

Table 1. Specifications of the Plug-Flow–Type Hollow-Fiber Membrane Reactor

Cutoff molecular mass	13,000
ID of ultrafiltration hollow-fiber tube	0.8 mm
OD of ultrafiltration hollow-fiber tube	1.4 mm
ID of shell tube	1.0 cm
Effective length of fiber tube	30 cm
Number of fiber tubes packed	7
Liquid volume in shell side	20.3 mL
Liquid volume in tube side	1.06 mL
Total inner surface area of fiber tubes	52.8 cm^2
Material of hollow-fiber tubes	poly(acrylonitrile)

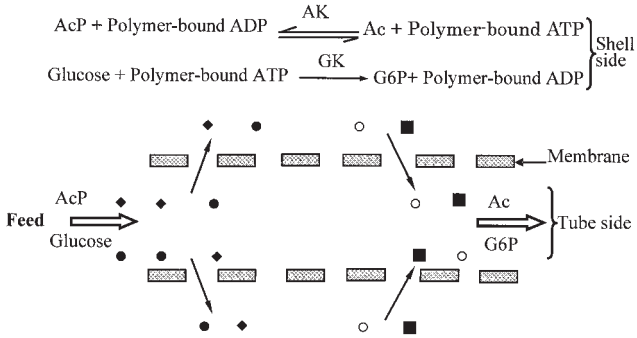

Figure 2. Illustrations of the transfer of the relevant components and overall reactions in G6P synthesis in the PFMR in a diffusion mode.

●: Glucose; ○: G6P; ◆: acetyl phosphate; ■: acetate.

cosubstrate AcP is supplied continuously into the hollow-fiber tubes as a feed. The substrate and cosubstrate supplied into the hollow-fiber tubes pass through the fiber membrane by diffusion into the shell-side space, where they react to produce G6P according to Eq. 1. This reaction is accompanied by the simultaneous regeneration of the polymer-bound ATP according to Eq. 2. The products G6P and acetate ions diffuse back into the reactant mixture stream in the tubes and are discharged from the reactor.

The following basic differential (Eqs. 5–8) and algebraic (Eqs. 9–12) equations for all the components in the G6P production and polymer-bound ATP regeneration in the reactor hold:

$$\frac{d\psi_1}{d\xi} = \frac{P_1 S}{Q}(\psi_1^* - \psi_1) = \frac{V_S}{QC_{1,f}}(-v_{GK}^*) \tag{5}$$

$$\frac{d\psi_2}{d\xi} = \frac{P_2 S}{Q}(\psi_2^* - \psi_2) = \frac{V_S}{QC_{1,f}}(v_{GK}^*) \tag{6}$$

$$\frac{d\psi_3}{d\xi} = \frac{P_3 S}{Q}(\psi_3^* - \psi_3) = \frac{V_S}{QC_{3,f}}(-v_{AK}^*) \tag{7}$$

$$\frac{d\psi_4}{d\xi} = \frac{P_4 S}{Q}(\psi_4^* - \psi_4) = \frac{V_S}{QC_{3,f}}(v_{AK}^*) \tag{8}$$

$$v_{AK}^* - v_{GK}^* = 0 \tag{9}$$

$$\psi_6^* = 1 - \psi_5^* \tag{10}$$

In the above equations, the subscripts 1, 2, 3, 4, 5, and 6 represent glucose, G6P, AcP, acetate, polymer-bound ATP, and polymer-bound ADP, respectively. v_{GK} and v_{AK} represent the rates of the reactions catalyzed by GK and AK, respectively, based on the concentrations in the shell-side space of the reactor. V_S represents the volume of the shell-side space, Q is the liquid flow rate, P_j (j = 1–4) is the permeability of component j, and ξ ($=Z/L$) is the dimensionless axial distance defined by the ratio of the distance Z from the reactor inlet to the total effective length L of hollow-fiber tubes. ψ_j and ψ_j^* (j = 1–6) are the dimensionless concentrations of components j in

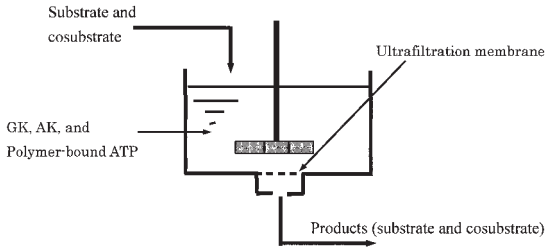

Figure 3. Illustration of the CSTMR in a filtration mode.

the tube side and in the shell-side space, respectively. The dimensionless concentration ψ_j is defined by

$$\psi_1 = C_1/C_{1,f} \qquad \psi_2 = C_2/C_{1,f} \qquad \psi_3 = C_3/C_{3,f}$$
$$\psi_4 = C_4/C_{3,f} \qquad \psi_5 = C_5/C_{5,f} \qquad \psi_6 = C_6/C_{5,f} \quad (11)$$

$C_{j,f}$ (j = 1, 3, and 5) expresses the concentration of component j in the feed solution and C_j (j = 1–6) represents the concentration of component j in the tube. The initial conditions are given by

$$\xi = 0 \qquad \psi_1 = \psi_3 = 1 \qquad \psi_2 = \psi_4 = 0 \qquad (12)$$

When the dimensionless concentrations ψ_1, ψ_2, ψ_3, and ψ_4, in the tube are known [from the initial condition (Eq. 12)], the dimensionless concentrations ψ_1^*, ψ_2^*, ψ_3^*, ψ_4^*, ψ_5^*, and ψ_6^*, in the shell can be determined from Eqs. 5 to 8 and checked through mass balance of Eqs. 9 and 10 for ADP–ATP reactions in the shell by using a trial-and-error method. Further, the dimensionless concentrations ψ_1, ψ_2, ψ_3, and ψ_4, in the tube can be obtained from Eqs. 5–8 from mass balance in the tube. To do so, an iterative procedure was used in the simulation program. At first, the concentrations in the shell at $\xi = 0$ were calculated with the initial conditions given by Eq. 12 by using bisectional and successive iterative methods. Next, the resultant concentrations in the shell and the initial concentrations in the tube were substituted in Eqs. 5 to 8 for mass balance in the tube to obtain concentration gradients in the axial direction at $\xi = 0$. Further, numerical solutions for slightly downward concentrations in the tube were obtained on the basis of the Runge–Kutta–Gill method. The process repeated itself to calculate the concentration profiles in the axial direction.

With respect to the permeability, the values P_j (j = 1–6), reported in our previous work,[9] were used for the simulation.

We also compared the results in the case of using polymer-bound ATP and ADP obtained in this study with those obtained in our previous work[9] in the case of using native ATP under the same conditions.

Continuous Stirred Tank–Type Membrane Reactor in a Filtration Mode. Figure 3 shows a schematic illustration of the CSTMR in a filtration mode. The transfer of the components involved in the reactions and the overall reactions in the reactor are shown schematically in Figure 4. Substrate, cosubstrate, and products can pass through the membrane, whereas the enzymes and the polymer-bound cofactors cannot pass through the membrane. Substrate and cosubstrate are supplied continuously to the reactor, and the net result is of a continuous stirred tank reactor with essentially constant enzyme and polymer-bound cofactor concentrations. Therefore, the mass balances of all the components were set up for a continuous stirred tank reactor based on the following assumptions: (1) steady-state condition is maintained, (2) the reaction mixture in the reactor is completely mixed, and (3) the concentrations of the substrate, cosubstrate, and products in the filtrate are the same as those in the reactor. Accordingly, the material balances for the present reaction system at the steady state can be expressed as follows:

$$\psi_1 = 1 - \frac{V_S}{QC_{1,f}}(v_{GK}) \qquad (13)$$

$$\psi_3 = 1 - \frac{V_S}{QC_{3,f}}(v_{AK}) \qquad (14)$$

$$v_{AK} - v_{GK} = 0 \qquad (15)$$

$$\psi_2 = 1 - \psi_1 \qquad (16)$$

$$\psi_4 = 1 - \psi_3 \qquad (17)$$

$$\psi_6 = 1 - \psi_5 \qquad (18)$$

where V_S is the liquid volume of the CSTMR.

Simulation Results and Discussion

Comparison of the performance of the PFMR in a diffusion mode with that of the CSTMR in a filtration mode

To compare the performances of the PFMR in diffusion mode and the CSTMR in filtration mode, we simulated both reactors assuming polymer-bound cofactors were used in both reactor types with having the same kinetic parameters as native ATP.

Figures 5–7 show the simulation results as a comparison between the performances of the PFMR in a diffusion mode and CSTMR in a filtration mode under various operational conditions. Figure 5 shows the effect of the flow rate under

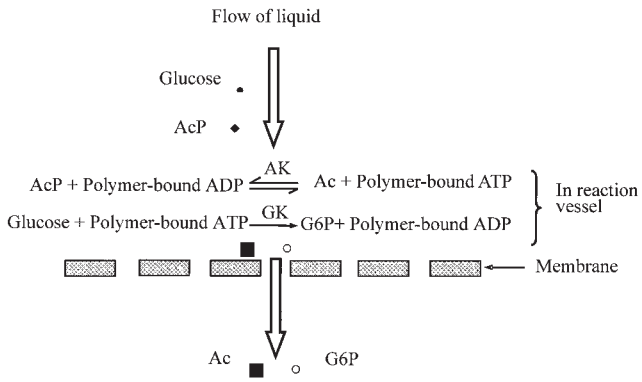

Figure 4. Illustration of the transfer of components and overall reactions of G6P synthesis in the CSTMR in a filtration mode.

●: Glucose; ○: G6P; ◆: acetyl phosphate; ■: acetate.

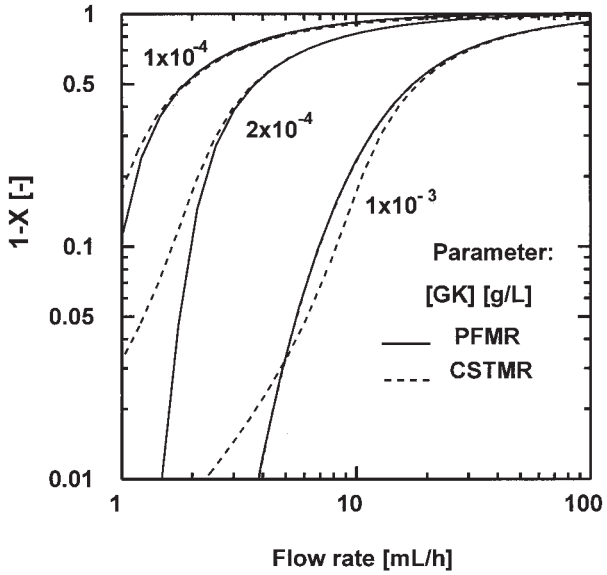

Figure 5. Effects of the liquid flow rate and GK concentration on the performances of the PFMR in a diffusion mode and the CSTMR in a filtration mode.

GK concentration ranged from 1×10^{-4} to 1×10^{-3} g/L with [AK]/[GK] = 10. Inlet concentrations of glucose, acetyl phosphate, and polymer-bound ATP were 10, 20, and 0.01 mM, respectively.

various GK concentrations on the reactor performance presented as the degree of glucose conversion ($1 - x$). As can be seen in the figure, the PFMR was superior to the CSTMR under low flow rate conditions when the enzyme concentrations are low. However, the CSTMR was slightly better than the PFMR when the enzyme concentration is high. Under this condition the latter reactor is controlled by diffusion of the substrate and cosubstrate.

Figure 6 shows the effects of the polymer-bound ATP concentration and the permeability of the substrate, cosubstrate, and product on the performance of the PFMR and CSTMR at two different flow rates. The simulation results showed that the glucose conversion in the PFMR increased with the permeability in the region of the diffusion control and that the permeability obviously had no effect on the performance of the CSTMR because the latter reactor was operated in a filtration mode. Furthermore, at a low flow rate ($Q = 2$ mL/h) the PFMR was found to be superior to the CSTMR, when the permeability value was equal to or higher than the value of the presently available ultrafiltration membrane. However, under a high flow rate condition of 5 mL/h the CSTMR is superior to the PFMR, when the permeability value was equal to or lower than the value of the presently available ultrafiltration membrane.

Figure 7 shows the effect of the molar concentration ratio of AcP to glucose in the feed solution on the reactor performance. The simulation elucidated that at low concentration ratios of AcP to glucose there was no significant difference in the reactor performances of either the PFMR or the CSTMR. However, when the ratio [AcP]/[Glucose] was ≥ 1 the PFMR was pronounced to have a better reactor performance than that of the CSTMR. Therefore, from a practical perspective, an excess amount of AcP should be supplied to the reactor. The amount should be determined by taking into consideration the residence time of the feed solution in the reactor and the decomposition rate of AcP.

Several investigators[7,8,13,14,27] reported that the CSTMR in a filtration mode used for enzymatic syntheses suffered from several drawbacks such as: (1) concentration polarization arising from the enzyme accumulation onto the membrane surface, which leads to a decrease in both the permeate flux and the enzyme activity; (2) rapid loss of the enzymatic activity resulting from the shear stress by means of the stirrer; (3) enzyme leakage resulting from the excessively high pressure; (4) low flux of liquid across the membrane; and (5) the need of ultrafiltration quality for the feed solution to prevent the accumulation of high molecular mass impurities in the reactor. In comparison, the only problem encountered in the PFMR in a diffusion mode is the influence of the mass transfer resistance on the reaction. Such resistance usually cannot be neglected. However, if a good membrane with higher permeabilities for substrates and products is available, the PFMR in a diffusion mode exhibits higher performance under a wide reaction and

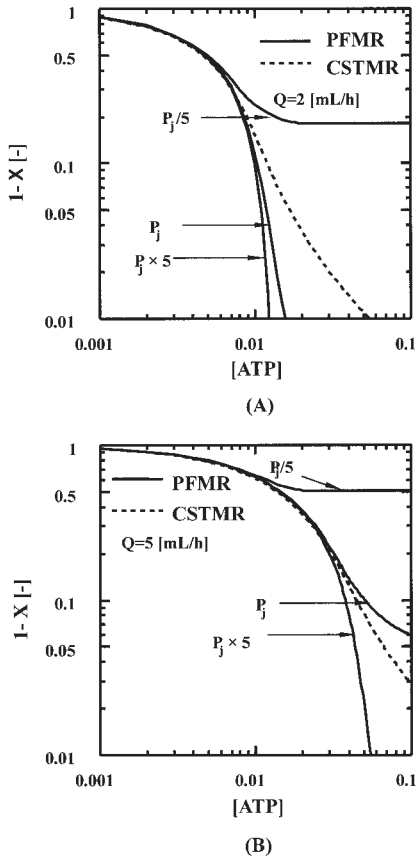

Figure 6. Effects of the polymer-bound ATP concentration and the permeability of the substrate, cosubstrate, and products on the performances of the PFMR in a diffusion mode and the CSTMR in a filtration mode at two different flow rates.

Liquid flow rates were (A) 2 mL/h and (B) 5 mL/h. GK concentration was 2×10^{-4} g/L and [AK]/[GK] = 10. Inlet concentrations of glucose and acetyl phosphate were 10 and 20 mM, respectively.

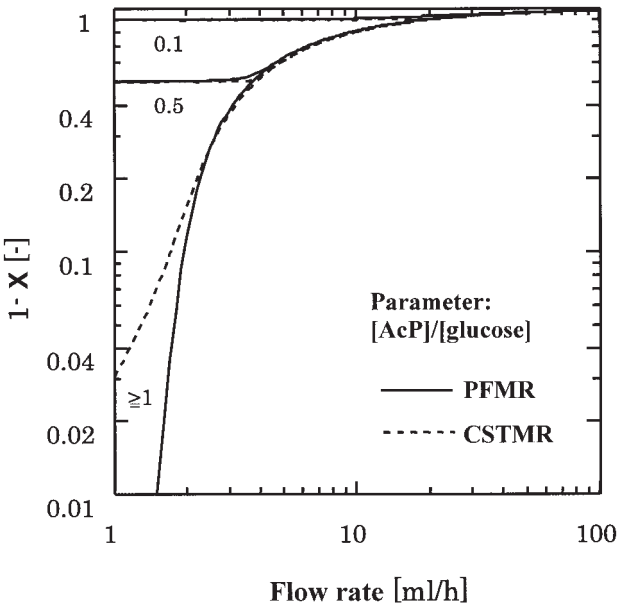

Figure 7. Effects of the molar concentration ratio of AcP to glucose in the feed solution on the performances of the PFMR in a diffusion mode and the CSTMR in a filtration mode.

GK concentration was 2×10^{-4} g/L and [AK]/[GK] = 10. Concentrations of glucose, acetyl phosphate, and polymer-bound ATP at the reactor inlet were 10, 20, and 0.01 mM, respectively.

operational conditions compared to the CSTMR in a filtration mode. In short, by taking into consideration the operational advantages and disadvantages of both reactor systems, it can be concluded that the PFMR in a diffusion mode is superior to the CSTMR in a filtration mode. This conclusion agrees with that obtained by Prenosil and Hediger,[7,8] who investigated an unisubstrate reaction system. They compared the performances of the CSTMR in a filtration mode and the PFMR in a diffusion mode for lactose hydrolysis catalyzed by β-galactosidase, in which the reaction obeys Michaelis–Menten kinetics with product inhibition. They concluded that with respect to an economical degree of conversion (<75%), the PFMR was superior to the CSTMR.

According to the above results and discussions, we decided to use the PFMR in a diffusion mode in the following theoretical analysis of the G6P production.

Comparison of the performances of the PFMR in a diffusion mode when native and polymer-bound ATPs were used

When native ATP is used as a cofactor, it is supposed that a feed solution containing the substrate glucose, cosubstrate acetyl phosphate, and native cofactor ATP with a low concentration is continuously supplied to the tube side, whereas both the AK and GK are confined within the shell side. On the other hand, when the polymer-bound ATP is used as a cofactor, it is supposed that a feed solution containing glucose and acetyl phosphate is continuously supplied to the tube side, whereas the polymer-bound ATP and both AK and GK are confined within the shell side.

Figure 8 compares the performance of the PFMR in a diffusion mode obtained using the polymer-bound ATP (assuming 100% relative activity and having the same kinetic parameters of native ATP) as a cofactor with that obtained using native ATP, which was reported by Ishikawa et al.[9] as a plot of the conversion vs. GK concentration with the flow rate Q as a parameter. The results show that the glucose conversion increases with the GK concentration and attains 100% when Q is small. However, the conversion attains constant values that are <100% when Q is large. This is because the diffusion of the substrate and cosubstrate through the fiber membrane becomes the controlling step when the GK concentration is high. It was expected that under the diffusion control conditions the glucose conversion that was attainable using the polymer-bound ATP was much higher than that using native ATP because confining the polymer-bound ATP in the shell-side space decreases the diffusion resistance of the cofactor. Unexpectedly, however, both cases were identical. To explore this unanticipated result the effects of the permeability of each substrate and cosubstrate were studied separately.

Figure 9 shows the effect of the permeability of each substrate and cosubstrate on the glucose conversion when native ATP is used as a cofactor. In this case, the permeability of the tested component was varied, whereas the permeabilities of the other components were kept as actual values reported in our previous work.[9] Figure 9A shows that a fivefold increase ($P_G \times 5$) or decrease ($P_G/5$) in the permeability of glucose had a remarkable effect on the glucose conversion. Figure 9B shows that only a fivefold decrease ($P_{AcP}/5$) in the permeability of acetyl phosphate has a considerable effect on the glucose conversion. As shown in Figure 9C, the ATP permeability was found to have no effect under its tested range. These results explained why confining ATP within the shell-side space had

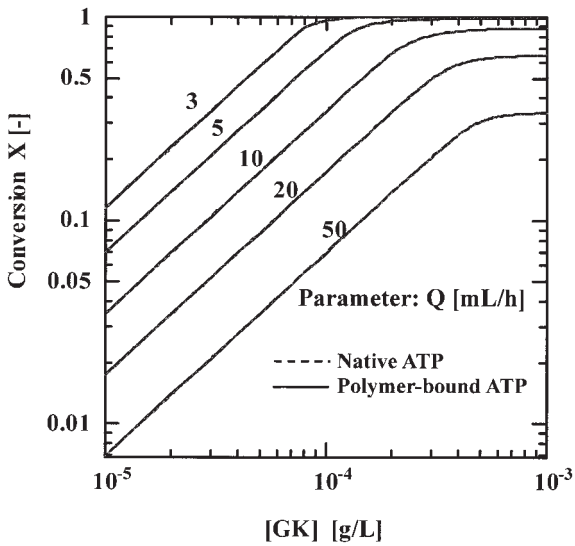

Figure 8. Comparison of the reactor performances obtained using native and polymer-bound ATPs in the PFMR in a diffusion mode.

Effects of the GK concentration and liquid flow rate Q on the glucose conversion are shown. Concentrations of glucose, acetyl phosphate, and native ATP or polymer-bound ATPs at the reactor inlet were 10, 20, and 0.1 mM, respectively, and [AK]/[GK] = 10.

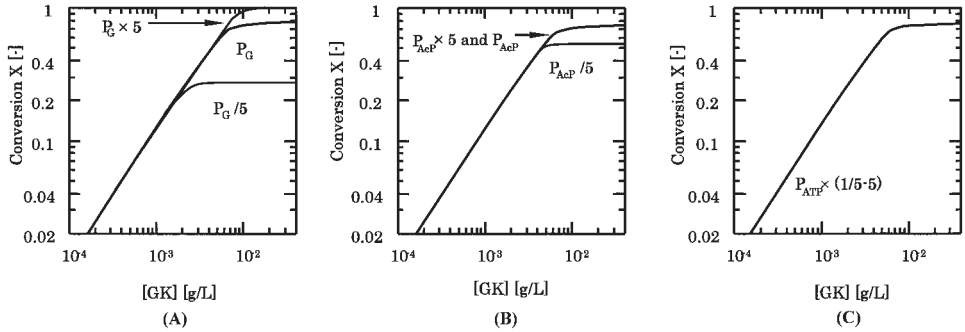

Figure 9. Effect of the permeability of each substrate and cosubstrate on the glucose conversion in the PFMR in a diffusion mode.

(A), (B), and (C) show the effect of the permeability of glucose, acetyl phosphate, and native ATP, respectively. Concentrations of glucose, acetyl phosphate, and native ATP at the reactor inlet were 10, 20, and 0.01 mM, respectively, and [AK]/[GK] = 10.

no significant effect on the glucose conversion. The phenomenon could be explained by the compensation of any decrease in the ATP concentration in the shell-side space by the regeneration reaction catalyzed by AK (reaction 2). This speculation can be proved by studying the effect of permeability of native ATP under the condition of no ATP regeneration (AK concentration is zero).

Figure 10 shows the effect of the permeability of native ATP on the reactor performance under no ATP regeneration conditions. As can seen in the figure, the increase (fivefold or more) in the ATP permeability increases the glucose conversion up to a limiting value, which is more than twofold of the value attainable using the actual ATP permeability, and decreasing permeability substantially decreases the glucose conversion. Such a result proves that the effect of ATP permeability takes place only under a no-regeneration condition, and that the ATP permeability will have no effect when ATP is regenerated by the reaction catalyzed by AK.

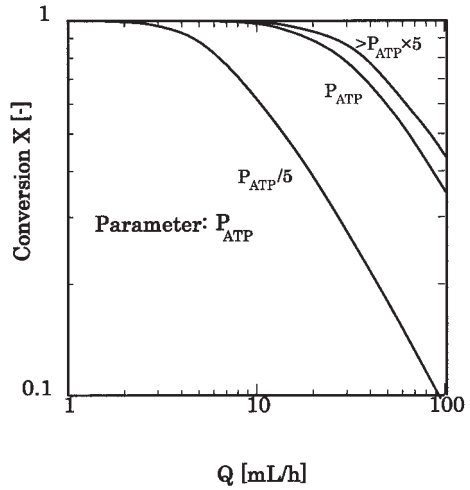

Figure 10. Effect of the permeability of native ATP on the glucose conversion under no ATP regeneration conditions in the PFMR in a diffusion mode.

Enzyme concentrations were 2×10^{-2} g/L GK and 0.0 g/L AK. Concentrations of glucose, acetyl phosphate, and native ATP at the reactor inlet were 10, 20, and 10 mM, respectively.

To analyze the results shown in Figure 8 more deeply, the concentration profiles of native ATP and ADP in the shell-side space were calculated theoretically under different [AK]/[GK] ratio conditions. As shown in Figure 11, the ATP concentration varies along with the reactor axis depending on the [AK]/[GK] ratio, but converges into a single value (the maximum value) at the reactor mid distance, irrespective of the [AK]/[GK] value. This constant ATP concentration was attained by the regeneration reaction catalyzed by AK. This constant ATP concentration was responsible for abrogating the effect of the mass transfer on the conversion. To confirm the role of the regeneration reaction on nullifying the effect of mass transfer on the conversion, the ratio of the rate v_{AK} of the ATP regeneration reaction catalyzed by AK (reaction 2) to the rate v_{GK} of the G6P synthesis reaction catalyzed by GK (reaction 1) under various [AK]/[GK] ratio conditions using native ATP was studied along with the axis of the reactor. Figure 12 shows the ratio v_{AK}/v_{GK} along with the axis of the reactor with the [AK]/[GK] ratio as the parameter using native ATP. As can be seen in the figure, when [AK]/[GK] > 0.1, the reaction rates, v_{AK} and v_{GK}, are almost equal at any point in the reactor.

Figure 13 shows the effects of the flow rate and the concentration of native ATP (dashed lines) or the polymer-bound ATP

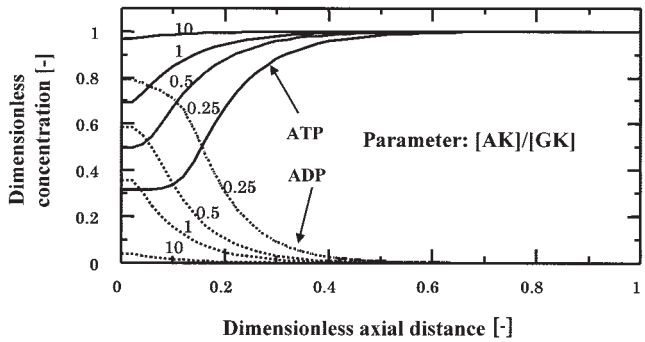

Figure 11. Concentration profiles of native ATP and ADP in the shell-side space in the PFMR in a diffusion mode under various [AK]/[GK] ratio conditions.

GK concentration was 0.1 g/L. Concentrations of glucose, acetyl phosphate, and native ATP at the reactor inlet were 10, 20, and 0.001 mM, respectively, at $Q = 5$ mL/h.

(solid lines) on the recycle number (total moles of G6P produced ÷ moles of ATP used) and the conversion of glucose in the PFMR in a diffusion mode. Under the conditions specified in the figure, both cases that use native ATP and the polymer-bound ATP gave the same conversion. However, the recycle number of the enzymes and the polymer-bound ATP attained 500,000 instead of 2000 for that of native ATP. These calculations were based on the assumption that the reactor was continuously operated for 1 month without the activity loss of the enzymes and polymer-bound ATP. This assumption is valid when the highly stable *B. stearothermophilus* GK and AK and the highly stable polymer-bound ATP prepared in our previous work[23] are used. Moreover, based on the simple polymer-bound ATP synthesis procedures developed in our previous work,[23] it becomes possible to overcome the cost barrier of the polymer-bound ATP synthesis, which is more advantageous for using polymer-bound ATP in the case of G6P production requiring ATP as a cofactor.

Based on the above results of theoretical calculations, it can be concluded that the performance of the PFMR in a diffusion mode becomes superior when the polymer-bound ATP is used instead of native ATP. This conclusion was derived by assuming that the same rate equations and same kinetic parameters could be used irrespective of the types of cofactors, native cofactors, and the polymer-bound cofactors. However, final judgment should be made by taking into consideration the differences in the cost and stability of the two types of cofactor and the kinetic parameters of the rate equations.

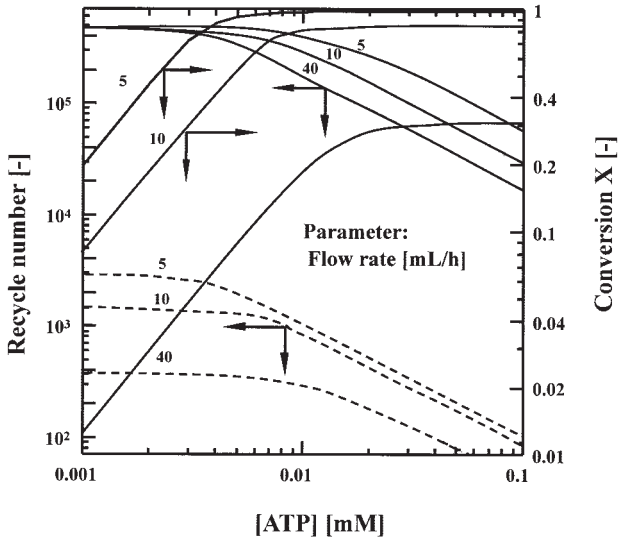

Figure 13. Effects of the flow rate and the concentration of native ATP (dashed lines) or the polymer-bound ATP (solid lines) on the recycle number and the conversion of glucose in the PFMR in a diffusion mode.

GK concentration was 12.8×10^{-4} g/L. Concentrations of glucose, acetyl phosphate, and native or polymer-bound ATPs at the reactor inlet were 10, 20, and 0.01 mM, respectively.

Notation

[AK] = concentration of acetate kinase, M
C_j = concentration of component j, M
[GK] = concentration of glucokinase, M
L = total effective length of hollow-fiber reactor, cm
P_j = permeability of component j through fiber membrane, m s^{-1}
Q = volumetric flow rate of the feed solution, mL h^{-1}
x = degree of glucose conversion
S = total inner surface area of fiber tubes, cm^2
v_{GK} = rate of the reactions catalyzed by GK, M^{-1} s^{-1}
v_{AK} = rate of the reactions catalyzed by AK, M^{-1} s^{-1}

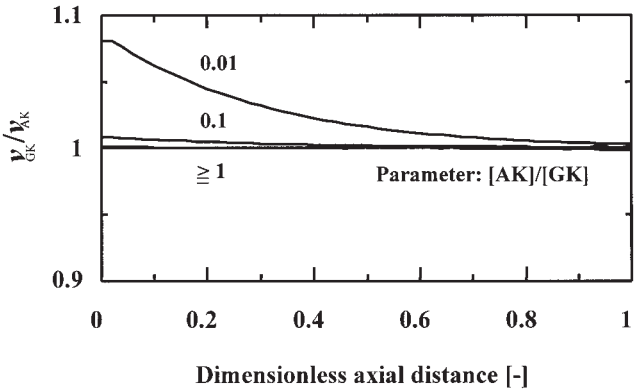

Figure 12. Ratio v_{GK}/v_{AK} along with the axis of the PFMR in a diffusion mode under several [AK]/[GK] ratio conditions.

GK concentration was 1×10^{-3} g/L. Concentrations of glucose, acetyl phosphate, and native ATP at the reactor inlet were 10, 20, and 0.01 mM, respectively, at Q = 5 mL/h.

V_S = liquid volume in the shell side, mL
Z = distance from the reactor inlet, cm

Greek letters

ξ = dimensionless axial distance from reactor inlet (=Z/L)
ψ = dimensionless concentration defined by Eq. 11
λ = kinetic parameter in Eq. 3
ω_j = kinetic parameter in Eq. 3
α_j = kinetic parameter in Eq. 4
β_j = kinetic parameter in Eq. 4

Subscripts

f = value in the feed solution
1 = glucose (substrate)
2 = G6P
3 = acetyl phosphate (cosubstrate)
4 = acetate
5 = ATP or polymer-bound ATP
6 = ADP or polymer-bound ADP
* = shell-side space

Literature Cited

1. Langer RS, Hamilton BK, Gardner CR, Archer MC, Colton CK. Enzymatic regeneration of ATP: I. Alternative routes. *AIChE J.* 1976; 22:1079-1090.
2. Langer RS, Hamilton BK, Gardner CR, Archer MC, Colton CK. Enzymatic regeneration of ATP: II. Equilibrium studies with acetate kinase and adenylate kinase. *AIChE J.* 1977;23:1-10.
3. Belfort G. Membrane and bioreactors: A technical challenge in biotechnology. *Biotechnol Bioeng.* 1989;33:1047-1066.
4. Prazeres DMF, Cabral JMS. Enzymatic membrane bioreactors and their applications. *Enzyme Microb Technol.* 1994;16:738-749.
5. Nidetzky B, Haltrich D, Kulbe KD. Carry out coenzyme conversion economically. *Chemtechnology.* 1996;26:31-36.
6. Nidetzky B, Neuhauser W, Haltrich D, Kulbe KD. Continuous enzy-

matic production of xylitol with simultaneous regeneration in a charged membrane reactor. *Biotechnol Bioeng.* 1996;52:387-396.
7. Prenosil JE, Hediger T. On membranes and membrane processes. Proc of Europe–Japan Congress, Streasa, Italy, Jun. 18–22; 1984.
8. Prenosil JE, Hediger T. *Membranes and Membrane Processes*. Drioli E, Nakagaki M, eds. New York, NY: Plenum; 1986.
9. Ishikawa H, Takase S, Tanaka T, Hikita H. Experimental investigation of G6P production and simultaneous ATP regeneration by conjugated enzymes in an ultrafiltration hollow-fiber reactor. *Biotechnol Bioeng.* 1989;34:369-379.
10. Ishikawa H, Tanaka T, Takase S, Hikita H. Theoretical analysis of G6P production and simultaneous ATP regeneration by conjugated enzymes in an ultrafiltration hollow-fiber reactor. *Biotechnol Bioeng.* 1989;34:369-379.
11. Widjaja A, Ogino H, Yasuda M, Ishimi K, Ishikawa H. Experimental investigation of fructose 1,6-diphsphate production and simultaneous ATP regeneration by conjugated enzymes in an ultrafiltration hollow-fiber reactor. *J Biosci Bioeng.* 1999;88:640-645.
12. Widjaja A, Shiroshima M, Yasuda M, Ogino H, Nakajima H, Ishikawa H. Enzymatic synthesis of fructose 1,6-diphosphate with ATP regeneration in a batch reactor and a semibatch reactor using purified enzymes of *Bacillus stearothermophilus. J Biosci Bioeng.* 1999;87: 611-618.
13. Fujii T, Miyawaki O, Yano T. Modeling of hollow-fiber capillary reactor for the production of L-alanine with coenzyme regeneration. *Biotechnol Bioeng.* 1991;38:1166-1172.
14. Berke W, Schuz H, Wandrey C, Morr M, Denda G, Kula M. Continuous regeneration of ATP in enzyme membrane reactor for enzymatic syntheses. *Biotechnol Bioeng.* 1988;32:130-139.
15. Prenosil JE, Hediger T. Performance of membrane fixed biocatalyst reactions. I: Membrane reactor system and molding. *Biotechnol Bioeng.* 1988;31:913-921.
16. Jones SKC, Yang RYK, White ETA. Novel hollow-fiber reactor with reversible immobilization of lipase. *AIChE J.* 1988;34:293-304.
17. Howaldt M, Kulbe KD, Chmiel HA. Continuous enzyme membrane reactor retaining the native nicotinamide cofactor NAD (H). *Ann NY Acad Sci.* 1990;589:253-260.
18. Ikemi M, Koizumi N, Ishimatsu Y. Sorbitol production in charged membrane bioreactor with coenzyme regeneration system: I. Selective retention of NADP (H) in a continuous reaction. *Biotechnol Bioeng.* 1990a;36:149-155.
19. Ikemi M, Ishimatsu Y, Kise S. Sorbitol production in charged membrane bioreactor with coenzyme regeneration system: II. The theoretical analysis of a continuous reaction retained and regenerated NADP (H). *Biotechnol Bioeng.* 1990b;36:155-165.
20. Ishikawa H, Maeda T, Hikita H. Initial-rate studies of a thermophilic glucokinase from *Bacillus stearothermophilus*. *Biochem J.* 1987;248: 13-20.
21. Shiroshima M, Widjaja A, Yasuda M, Ogino H, Ishimi K, Ishikawa H. Theoretical investigation of fructose 1,6-diphsphate production and simultaneous ATP regeneration by conjugated enzymes in an ultrafiltration hollow-fiber reactor. *J Biosci Bioeng.* 1999;88:632-639.
22. Ishikawa H, Shiroshima M, Widjaja A, Nakajima H, Tsurutani R. Kinetics and mechanism of acetate kinase from *Bacillus stearothermophilus. J Chem Eng Jpn.* 1995;28:517-524.
23. Abdelmoez W, Yasuda M, Ogino H, Ishimi K, Ishikawa H. Synthesis of new polymer-bound adenine nucleotides using starburst PAMAM dendrimers. *Biotechnol Prog.* 2002;18:706-712.
24. Abdelmoez W, Bobe I, Ishimi K, Ishikawa H. Kinetics of the reaction catalyzed by thermophilic glucokinase from *Bacillus stearothermophilus* using the carboxy-terminated PAMAM-bound adenine nucleotides as cofactors. *Biochem Eng J.* 2004;20:35-38.
25. Abdelmoez W, Ishimi K, Bobe I, Ishikawa H. Investigation of glucose 6-phosphate production and simultaneous carboxy-terminated PAMAM-bound adenine nucleotides regeneration by conjugated enzymes in a batch reactor. *J Chem Eng Jpn.* 2004;37:1303-1309.
26. Mansson M, Mosbach K. Immobilized active coenzymes. *Methods Enzymol.* 1987;136:1-8.
27. Kragl U, Vasic-Rack D, Wandrey C. Continuous processes with soluble enzymes. *Indian J Chem.* 1993;32B:103-117.

Manuscript received Feb. 18, 2005, and revision received Jun. 29, 2005.